Synapse Elimination and Learning Rules Coregulated by Major Histocompatibility Class I Protein H2-D^b

Hanmi Lee, PhD,[1] Lowry A. Kirkby, PhD,[2]
Barbara K. Brott, PhD,[1] Jaimie D. Adelson, PhD,[1]
Sarah Cheng, BS,[1] Marla B. Feller, PhD,[2]
Akash Datwani, PhD,[1] and Carla J. Shatz, PhD[1]

[1]Departments of Biology and Neurobiology and Bio-X
The James H. Clark Center
Stanford, California

[2]Department of Molecular and Cell Biology
Helen Wills Neuroscience Institute
University of California, Berkeley
Berkeley, California

SfN Society for Neuroscience

NOTES

Introduction

The formation of precise connections between retina and LGN involves the activity-dependent elimination of some synapses and the strengthening and retention of others. Here we show that the major histocompatibility class I (MHCI) molecule H2-Db is necessary and sufficient for synapse elimination in the retinogeniculate system. In mice lacking both H2-Kb and H2-Db (KbDb–/–) despite intact retinal activity and basal synaptic transmission, the developmentally regulated decrease in functional convergence of retinal ganglion cell synaptic inputs to LGN neurons fails, and eye-specific layers do not form. Neuronal expression of just H2-Db in KbDb–/– mice rescues both synapse elimination and eye-specific segregation despite a compromised immune system. When patterns of stimulation mimicking endogenous retinal waves are used to probe synaptic learning rules at retinogeniculate synapses, long-term synaptic potentiation (LTP) is intact but long-term synaptic depression (LTD) is impaired in KbDb–/– mice. This change is the result of an increase in Ca^{2+}-permeable (CP) AMPA receptors. Restoring H2-Db to KbDb–/– neurons renders AMPA receptors Ca^{2+} impermeable and rescues LTD. These observations reveal an MHCI-mediated link between developmental synapse pruning and balanced synaptic learning rules enabling both LTD and LTP. They also demonstrate a direct requirement for H2-Db in functional and structural synapse pruning in CNS neurons.

Early in development before photoreceptors function, retinal ganglion cells (RGCs) spontaneously generate correlated bursts of action potentials called "retinal waves" (Meister et al., 1991; Wong et al., 1993; Feller et al., 1996). Postsynaptic LGN neurons in turn are driven to fire in similar patterns (Mooney et al., 1996; Weliky and Katz, 1999), and this endogenous activity is even relayed further into the visual system (Ackman et al., 2012). Although there is consensus that retinal waves and correlated activity are needed for RGC synapse remodeling and segregation of RGC axons into eye-specific layers (Penn et al., 1998; Huberman et al., 2008), little is known at synaptic or molecular levels about how natural patterns of activity are read out to drive elimination and structural remodeling prior to sensory experience. It is assumed that synaptic learning rules are present at retinogeniculate synapses and that implementation of these rules leads ultimately to either synapse stabilization or elimination. Efforts to discover molecular mechanisms of developmental synapse elimination have implicated several unexpected candidates, all with links to the immune system, including neuronal pentraxins, complement C1q, and MHCI family members (Huh et al., 2000; Bjartmar et al., 2006; Stevens et al., 2007). However, it is not known whether any of these molecules regulate plasticity rules at developing synapses. Moreover, because germline knock-out mice were examined in each of these examples, it is not known whether neuronal or immune function is required for synapse elimination *in vivo*. Here we examine these questions and test whether genetically restoring H2-Db expression selectively to CNS neurons *in vivo* can rescue synapse elimination in mice that nevertheless lack an intact immune system.

Defective Synapse Elimination in KbDb–/– LGN

MHCI genes *H2-Db* and *H2-Kb*, members of a polymorphic family of more than 50, are expressed in LGN neurons (Huh et al., 2000) and were discovered in an unbiased screen *in vivo* for genes regulated by retinal waves: Blocking this endogenous neural activity not only prevents RGC axonal remodeling (Penn et al., 1998) but also downregulates the expression of MHCI mRNA (Corriveau et al., 1998). Previous studies have suggested that MHCI molecules regulate synapse number in cultured neurons (Glynn et al., 2001) and are needed for anatomical segregation of RGC axons into LGN layers *in vivo* (Huh et al., 2000; Datwani et al., 2009). To examine whether H2-Kb and H2-Db are involved in functional synapse elimination, whole-cell microelectrode recordings were made from individual neurons in wild-type (WT) or KbDb–/– LGN slices (Fig. 1*a*) (Chen and Regehr, 2000; Hooks and Chen, 2006). Adult mouse LGN neurons normally receive strong monosynaptic inputs from one to three RGC axons, but in development, many weak synaptic inputs are present. The majority are eliminated between postnatal day 5 (P5) and P12 before eye opening, while the few remaining inputs strengthen, resulting in adult-like synaptic innervation by P24–P30 (Chen and Regehr, 2000). By gradually increasing optic tract (OT) stimulation intensity, individual RGC axons with progressively higher firing thresholds can be recruited (Chen and Regehr, 2000), generating a stepwise series of EPSCs recorded in each LGN neuron. For example, at P21 in WT mice, only two steps are present (Fig. 1*b*), indicating that just two RGC axons provide input to this LGN neuron, as expected. In contrast, in KbDb–/– LGN neurons, there are many EPSC steps (Fig. 1*c*), a pattern similar to that in much younger WT mice before synapse elimination (Chen and Regehr, 2000; Hooks and Chen, 2006).

To obtain more quantitative information, minimal stimulation was used to estimate single-fiber AMPA

NOTES

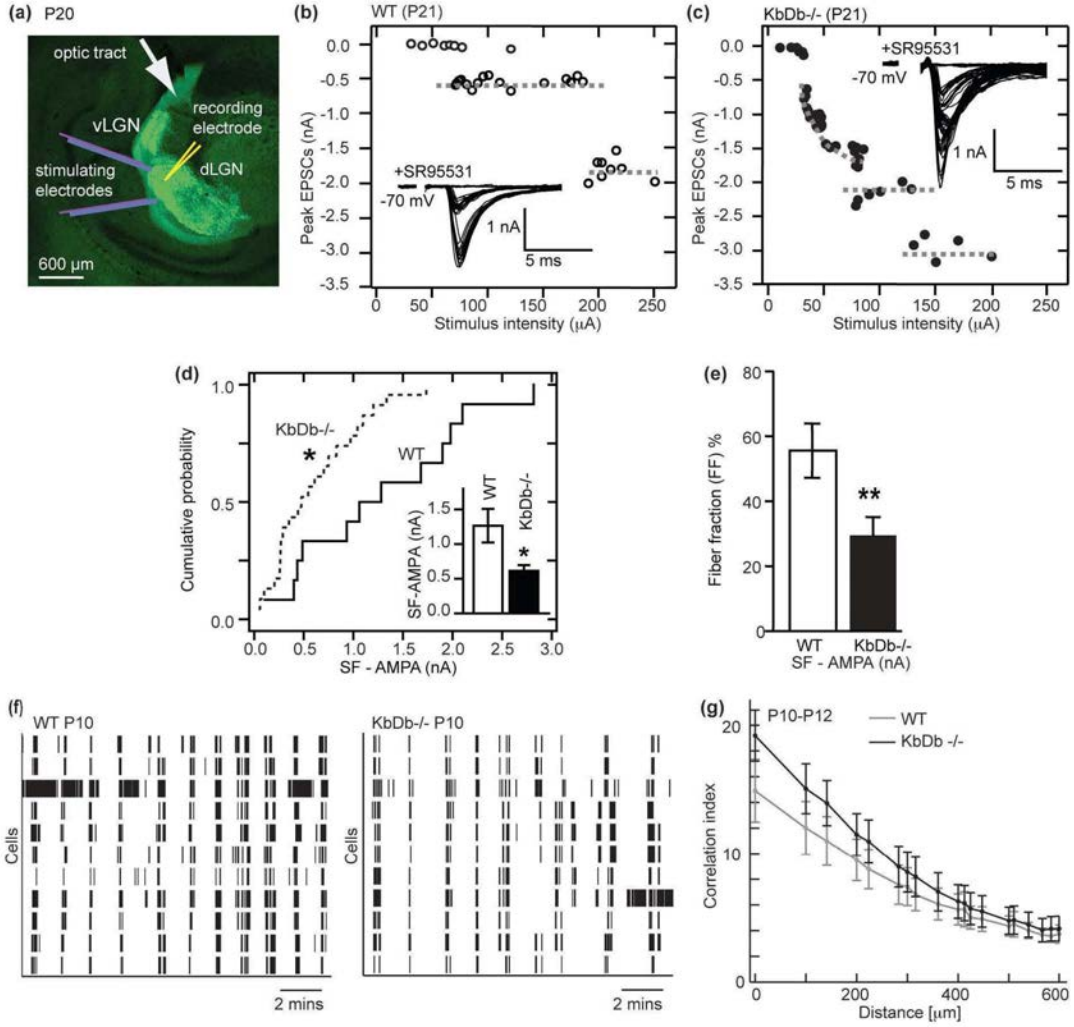

Figure 1. Failure of retinogeniculate synapse elimination despite intact retinal waves in KbDb–/– mice. ***a–e***, Impaired synapse elimination in KbDb–/– neurons at P20–P24. ***a***, Slice preparation used for whole-cell recording from dLGN neurons and stimulation of RGC axons in the OT. The retinogeniculate projection is visualized by injecting CTb AF488 (green) into the contralateral eye. Scale bar, 600 µm. ***b, c,*** EPSC amplitude versus OT stimulus intensity. Insets, example traces. ***d***, Cumulative probability histograms of SF-AMPA. Inset, mean ± SEM for WT mice (n = 12/N = 6); KbDb–/– mice (n = 23/N = 8); *$p < 0.05$. ***e,*** Fiber fraction (FF) for WT mice (n = 12/N = 6); KbDb–/– mice (n = 21/N = 8); **$p < 0.01$; *t*-test for ***d–g.*** Intact retinal waves in RGCs of KbDb–/– mice at P10–P12. ***f***, Raster plots of single-unit spike trains recorded from 10 representative RGCs during retinal waves. ***g***, Correlation indices vs interelectrode distance for all cell pairs for WT (N = 5) vs KbDb–/– mice (N = 6). Data correspond to mean values of medians from individual datasets, and error bars represent SEM. n = cells/N = animals; dLGN, dorsal lateral geniculate nucleus; vLGN, ventral lateral geniculate nucleus. Reprinted with permission from Lee H et al. (2014), Figure 1. Copyright 2014, Nature Publishing Group.

(SF-AMPA) strength (Stevens and Wang, 1994) (see Methods and Extended Data for Figs. 1*a*,*b*, available at https://www.ncbi.nlm.nih.gov/pmc/articles/PMC4016165). On average, the amplitude of SF-AMPA in KbDb–/– mice is almost half that of WT mice, and the cumulative probability distribution of EPSC amplitudes recorded from KbDb–/– LGN neurons is also consistent with the presence of smaller EPSCs (Fig. 1*d*) (note that onset latency of SF-AMPA is similar in both genotypes; Extended Data, Fig. 1*c*). In contrast, *maximal* synaptic input (Max-AMPA) does not differ between WT and KbDb–/– mice (Extended Data, Fig. 1*d*). Fiber fraction, an index of how much each input contributes to total synaptic response (Chen and Regehr, 2000) (Methods), is half as large in KbDb–/– mice as in WT mice (Fig. 1*e*), consistent with the idea that the number of RGC synapses in KbDb–/– LGN neurons is greater than in WT neurons. An alternative possibility—that differences can arise from altered probability of release—is unlikely because paired-pulse ratio (an index of presynaptic release probability) is similar in WT and KbDb–/– neurons

NOTES

at a variety of stimulus intervals (Extended Data, Figs. 1*e–h*). Together, these experiments, which directly measure the functional status of synaptic innervation, demonstrate that either or both H2-Kb and H2-Db are required for retinogeniculate synapse elimination.

Intact Retinal Wave Activity in KbDb–/– Mice

Many previous studies have shown that retinogeniculate synapse elimination and eye-specific segregation in LGN fail if retinal waves are blocked or perturbed (Feller et al., 1996; Penn et al., 1998; Huberman et al., 2008). Thus, waves could be absent or abnormal in KbDb–/– mice. To examine this possibility, waves were recorded using a multielectrode array to monitor action potential activity from many ganglion cells in KbDb–/– or WT retinas between P5 and P12—the peak period of extensive RGC synapse remodeling requiring waves. The spatiotemporal pattern of waves in KbDb–/– retina is indistinguishable from WT retina (Fig. 1*f*; Extended Data, Figs. 2*a–e*). Moreover, the correlation index between all RGC pairs (a measure of the distance over which cells fire together; Meister et al., 1991; Wong et al., 1993; Torborg et al., 2005) is almost identical (Fig. 1*g*; Extended Data, Fig. 2*a*). Retinal wave activity also transitioned normally from cholinergic-dependent stage II (P5–P8) to glutamatergic-dependent stage III (P10–P12) (Extended Data, Figs. 2*a–e*) (Huberman et al., 2008). After eye opening, vision in KbDb–/– mice is also normal (Datwani et al., 2009). Thus, synapse elimination and eye-specific segregation fail to occur despite intact retinal activity patterns in KbDb–/– mice, implying that one or both of these MHCI proteins acts downstream of activity to drive synapse remodeling.

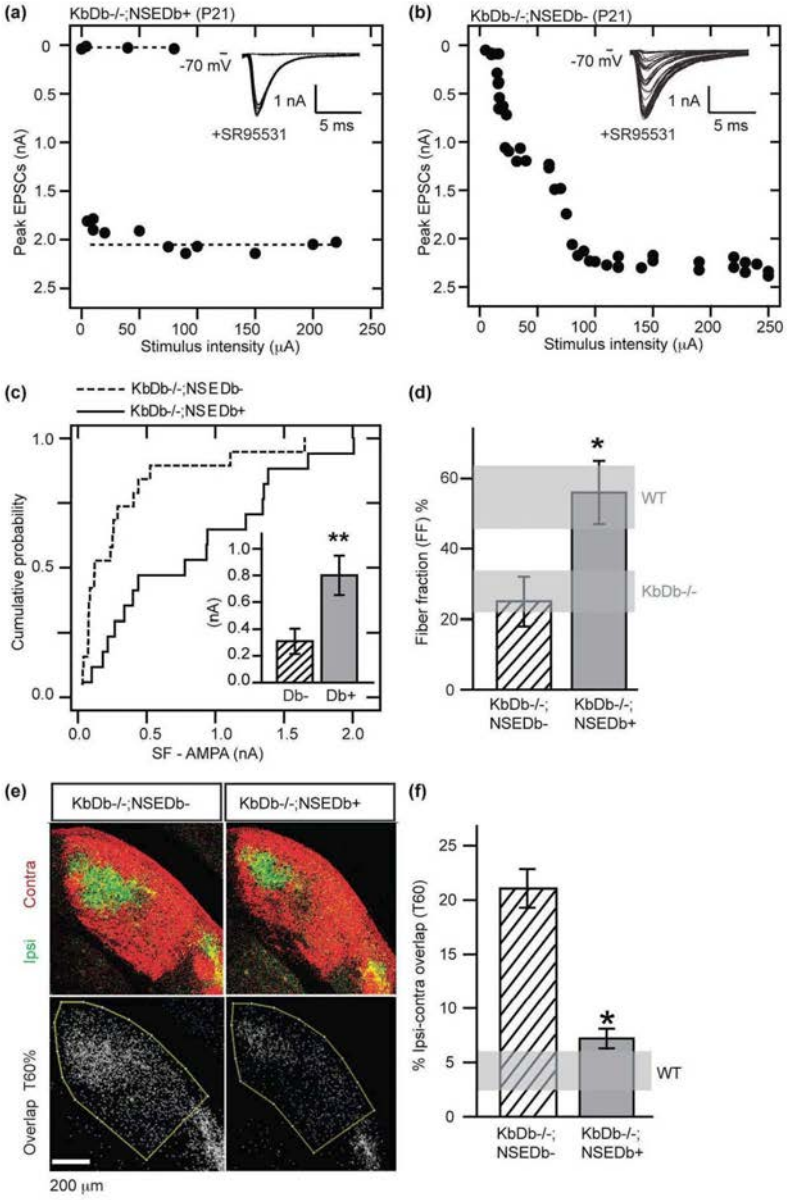

Figure 2. H2-Db expression in neurons rescues synapse elimination and eye-specific segregation in KbDb–/– LGN. ***a–d***, Rescue of synapse elimination at P20–P24. ***a,b,*** EPSC amplitudes vs OT stimulus intensity. Insets: example traces. ***c***, Cumulative probability histogram of SF-AMPA. Inset, mean ± SEM for control: Db– (KbDb–/–;NSEDb–; n = 19/N = 5). Rescue, Db+ (KbDb–/–;NSEDb+; n = 17/N = 7), $**p < 0.01$. ***d***, FF is also rescued in KbDb–/–;NSEDb+ mice (n = 16/N = 7) compared with KbDb–/–;NSEDb– animals (n = 18/N = 5); $*p < 0.05$; Mann–Whitney *U* test for ***c–d***. Horizontal gray bars delineate Fig. 1***e*** data (mean ± SEM). ***e, f,*** Rescue of eye-specific segregation in KbDb–/–;NSEDb+ mice at P34. ***e,*** Top, Coronal sections of dLGN showing pattern of retinogeniculate projections from the ipsilateral (green) and contralateral (red) eyes. Bottom, Region of ipsi-contra pixel (white) overlap between the two channels at 60% intensity threshold (T60%). Scale bar, 200 μm. ***f,*** Percentage of dLGN area occupied by ipsi-contra overlap. mean ± SEM for KbDb–/–;NSEDb– (N = 3) and KbDb–/–;NSEDb+ (N = 4) mice (T60%); $*p < 0.05$; 2-way ANOVA [Lee H et al, (2014) Extended Data, Fig. 5]. Horizontal gray bar indicates WT value at T60% (Datwani et al., 2009). n = cells/N = animals. Reprinted with permission from Lee H et al. (2014), Figure 2. Copyright 2014, Nature Publishing Group.

NOTES

Neuronal H2-Db Rescues Elimination and Segregation

H2-Db and H2-Kb are also critical for immune function and CD8 T-cell development (Vugmeyster et al., 1998). Both MHCI molecules are expressed in LGN during the period of retinogeniculate synaptic refinement, with H2-Db higher than H2-Kb (Huh et al., 2000; Datwani et al., 2009). To separate a contribution of the immune system, and to examine whether neuronal expression is sufficient for synapse elimination, H2-Db expression was restored exclusively to neurons by crossing KbDb–/– mice to NSEDb+ mice in which H2-Db expression is regulated under the neuron-specific enolase (NSE) promoter (Rall et al., 1995). "Rescued" offspring littermates have H2-Db expression restored to CNS neurons, while the rest of the body remains KbDb–/– (KbDb–/–; NSEDb+); "control" littermates (KbDb–/–; NSEDb–) lack H-2Kb and H2-Db everywhere (Extended Data, Fig. 3*a*). Genomic rescue as well as low but highly significant levels of H2-Db mRNA ($p = 0.0001$) and protein can be detected in KbDb–/–; NSEDb+ thalamus at P10 (Extended Data, Figs. 3*b–e*). In contrast, no H2-Db can be detected in spleen, gut, or liver, with little if any expression in retina, hippocampus, and cortex of KbDb–/–;NSEDb+ mice.

In KbDb–/–;NSEDb+ LGN neurons, only one to two EPSC steps could be evoked in response to increasing OT stimulus intensity (Fig. 2*a*), similar to the mature WT innervation pattern (compare Fig. 1*b*) but very different from littermate KbDb–/–;NSEDb– controls (Fig. 2*b*). Minimal stimulation also revealed an increase in SF-AMPA strength (Fig. 2*c*; Extended Data, Figs. 1*c*, 4*b*). Max-AMPA is similar between these genotypes (Extended Data, Fig. 4*a*); thus, fiber fraction in KbDb–/–;NSEDb+ LGN neurons is 56% versus 25% in KbDb–/–;NSEDb– neurons (Fig. 2*d*): strikingly similar to WT (cf. Fig. 1*e*). Therefore, expression of H2-Db in neurons rescues RGC synapse elimination in KbDb–/– LGN close to WT levels.

The formation of the adult anatomical pattern of eye-specific segregation in the LGN involves synapse elimination: Initially intermixed RGC axons from the right and left eyes remodel, eventually restricting their terminal arbors to the appropriate LGN layer (Shatz and Kirkwood, 1984; Shatz, 1996). To examine whether eye-specific segregation in the LGN is also rescued, anatomical tract-tracing methods (Torborg and Feller, 2004; Datwani et al., 2009) were used at P34, an age chosen because it is more than 3 weeks after segregation is normally complete as assessed anatomically. The retinogeniculate projections in LGN of KbDb–/–;NSEDb+ mice appear almost indistinguishable from WT mice, both in eye-specific pattern (Fig. 2*e*) and in the percentage of overlap between ipsilateral and contralateral projections (Fig. 2*f*; Extended Data, Figs. 5*a,b*). Segregation is impaired in control KbDb–/–;NSEDb– littermates (Fig. 2*e*), as expected from previous studies of KbDb–/– mice (Datwani et al., 2009). These anatomical results support the electrophysiological studies mentioned earlier and strongly suggest that both RGC synapse elimination and eye-specific segregation require neuronal H2-Db.

Impaired LTD with Natural Activity Patterns

Synapse elimination is thought to involve cellular processes leading to synaptic weakening such as LTD (Zhou et al., 2004; Bastrikova et al., 2008); conversely, LTP-like mechanisms are postulated to strengthen and stabilize synapses (Yuste and Bonhoeffer, 2001; Malenka and Bear, 2004). In addition, spike-timing-dependent mechanisms are crucial in *Xenopus* tectum for visually driven tuning of receptive fields (Mu and Poo, 2006). In mammalian LGN, LTP (Mooney et al., 1993) or LTD (Ziburkus et al., 2009) can be induced at retinogeniculate synapses using 100 Hz OT stimulation, which is far different from the endogenous bursting patterns generated by retinal waves (Figs. 1*f,g*) (Meister et al., 1991; Wong et al., 1993; Feller et al., 1996; Mooney et al., 1996). However, realistic patterns of OT stimulation mimicking waves, paired with postsynaptic depolarization of LGN neurons, have also been used. Results revealed a synaptic learning rule that generates LTP when presynaptic and postsynaptic activity coincide (Butts et al., 2007; Shah and Crair, 2008) but generates LTD when presynaptic OT activity precedes postsynaptic LGN depolarization within a broad window corresponding to the 60–90 s duty cycle of retinal waves (Figs. 3*a–c*; Extended Data, Fig. 2*b*) (Butts et al., 2007). Moreover, using these timing patterns in conjunction with optogenetic stimulation of retina is sufficient to either drive or prevent segregation of RGC axons, depending on the pattern (Zhang et al., 2011).

To determine whether synaptic learning rules based on natural activity patterns are altered at KbDb–/– retinogeniculate synapses, perforated patch recordings were made in LGN slices from WT versus KbDb–/– mice at P8–P13, the relevant period when extensive synapse elimination and eye-specific segregation are actually occurring. First, paired pulse stimulation was used to examine release probability: The same amount of synaptic depression was observed in WT and KbDb–/– mice, implying similar probabilities (Extended Data, Fig. 6). Next, synchronous activity

patterns were used in which 10 Hz OT stimulation was paired with LGN depolarization (Figs. 3*a*,*b*: 0 ms latency), generating 10–20 Hz bursts of action potentials in LGN neurons mimicking retinal waves (Mooney et al., 1996; Weliky and Katz, 1999). In WT neurons, synchronous stimulation induced LTP (Figs. 3*d*,*f*; 117% ± 8% over baseline; $p < 0.001$). In KbDb–/– LGN neurons, the same protocol elicited LTP indistinguishable from WT neurons (Figs. 3*e*,*f*).

In contrast, induction using asynchronous activity patterns reveals a defect in LTD. In WT mice, when OT stimulation precedes LGN neuron depolarization by 1.1 s (Figs. 3*a*,*c*: 1100 ms latency), LTD results (Figs. 3*g*,*i*: 12% decrease from baseline; $p < 0.001$). In contrast, in KbDb–/– mice, the same induction protocol failed to induce synaptic depression; if anything, a slight but significant potentiation was seen (Figs. 3*h*,*i*: 5% increase from baseline; $p < 0.005$). Thus, although LTD using asynchronous presynaptic and postsynaptic activity patterns is a robust feature of WT retinogeniculate synapses during the period of synapse elimination and eye-specific layer formation, it appears to be absent in KbDb–/– mice. This impairment is consistent with the failure of synapse elimination and axonal remodeling in KbDb–/– mice.

Ca^{2+}-Permeable AMPA Receptors at KbDb–/– Synapses

Impaired LTD in KbDb–/– mice could result from altered regulation of NMDA-receptor-mediated synaptic responses because LTP and LTD are known to depend on NMDA receptors at a variety of synapses (Malenka and Bear, 2004). Surprisingly, the NMDA:AMPA ratio did not differ between genotypes (Extended Data, Figs. 7*a*,*b*). However, the kinetics of I_{AMPA} recorded in KbDb–/– LGN neurons are markedly prolonged compared with WT neurons (Figs. 4*a*–*d*). The slowed decay in KbDb–/– EPSCs is unlikely to result from different peak I_{AMPA} amplitudes ($p > 0.1$) (Fig. 4*d*) but could occur if there were greater Ca^{2+} influx through AMPA receptors.

CP-AMPA receptors are blocked selectively by bath-applying the specific antagonist NASPM (1-naphthyl acetyl spermine), a synthetic homologue of Joro spider toxin (Liu and Cull-Candy, 2000). Indeed, in KbDb–/– LGN neurons, 100 µM NASPM blocked 40% of the current recorded at –70 mV but only 20% in WT neurons (Fig. 4*e*; Extended Data, Fig. 7*c*), confirming a twofold increase in CP-AMPA receptor–mediated currents in KbDb–/– neurons. Another diagnostic feature of CP-AMPA receptors is rectification in the current–voltage (I–V) relationship when spermine is present in the internal recording solution (Liu and Cull-Candy, 2000; Cull-Candy et al., 2006; Isaac et al., 2007). In WT neurons, the I–V relationship is linear; however in KbDb–/– LGN neurons, rectification is very prominent (Figs. 4*f*,*g*; Extended Data, Fig. 7*d*), though it can be linearized close to WT levels by bath application of NASPM (Figs. 4*f*,*g*). This implies that the prominent I–V rectification in KbDb–/– arises from an increase in CP-AMPA receptors.

Differences in composition of GluR subunits are known to modulate AMPA receptor Ca^{2+} permeability, and tetramers containing GluR2 confer Ca^{2+} impermeability (Cull-Candy et al., 2006). Indeed, the ratio of GluR1:GluR2, the most prevalent subunits (Hohnke et al., 2000; Cull-Candy et al., 2006; Goel et al., 2006), is slightly increased by 30% in developing thalamus from KbDb–/– mice ($p = 0.07$; Extended Data, Fig. 7*e*). The thalamus is highly heterogeneous, so we also examined cortical neuronal cultures: the ratio of GluR1:GluR2 also significantly increased by 230% in KbDb–/– mice ($p = 0.03$; Extended Data, Fig. 7*f*). Elevated levels of GluR1 subunits suggest that AMPA receptors in KbDb–/– mice are more likely to be composed of GluR1 homomers, yielding increased Ca^{2+} permeability. Together, these results point to an increase in CP-AMPA receptors in KbDb–/– mice. Similar increases in CP-AMPA receptors at other synapses are known to shift synaptic learning rules away from LTD and toward LTP (Jia et al., 1996; Toyoda et al., 2007). If so, the deficit in LTD observed with the asynchronous pairing protocol (Figs. 3*c*,*i*) in KbDb–/– LGN should be rescued using NASPM to block CP-AMPA receptors—exactly what was observed (Extended Data, Fig. 8).

Neuronal H2-Db Rescues Synaptic Function and LTD

If H2-Db affects synapse elimination by regulating the properties of AMPA receptors, then retinogeniculate EPSCs should be rescued to WT in the LGN of KbDb–/–;NSEDb+ mice. Indeed, the kinetics of IAMPA are significantly faster in KbDb–/–;NSEDb+ LGN neurons than in KbDb–/–;NSEDb– neurons (Figs. 5*a*–*c*; Extended Data, Fig. 9*a*), implying a decrease in CP-AMPA receptors. Accordingly, NASPM-dependent inhibition of I_{AMPA} is only 20% in KbDb–/–;NSEDb+ mice, significantly reduced from the 40% inhibition observed in littermate KbDb–/–;NSEDb– mice (Fig. 5*d*; Extended Data, Fig. 9*a*). Moreover, the I–V relationship is linearized in KbDb–/–;NSEDb+ LGN neurons when spermine is present in the internal recording solution, and bath application of NASPM has little additional

NOTES

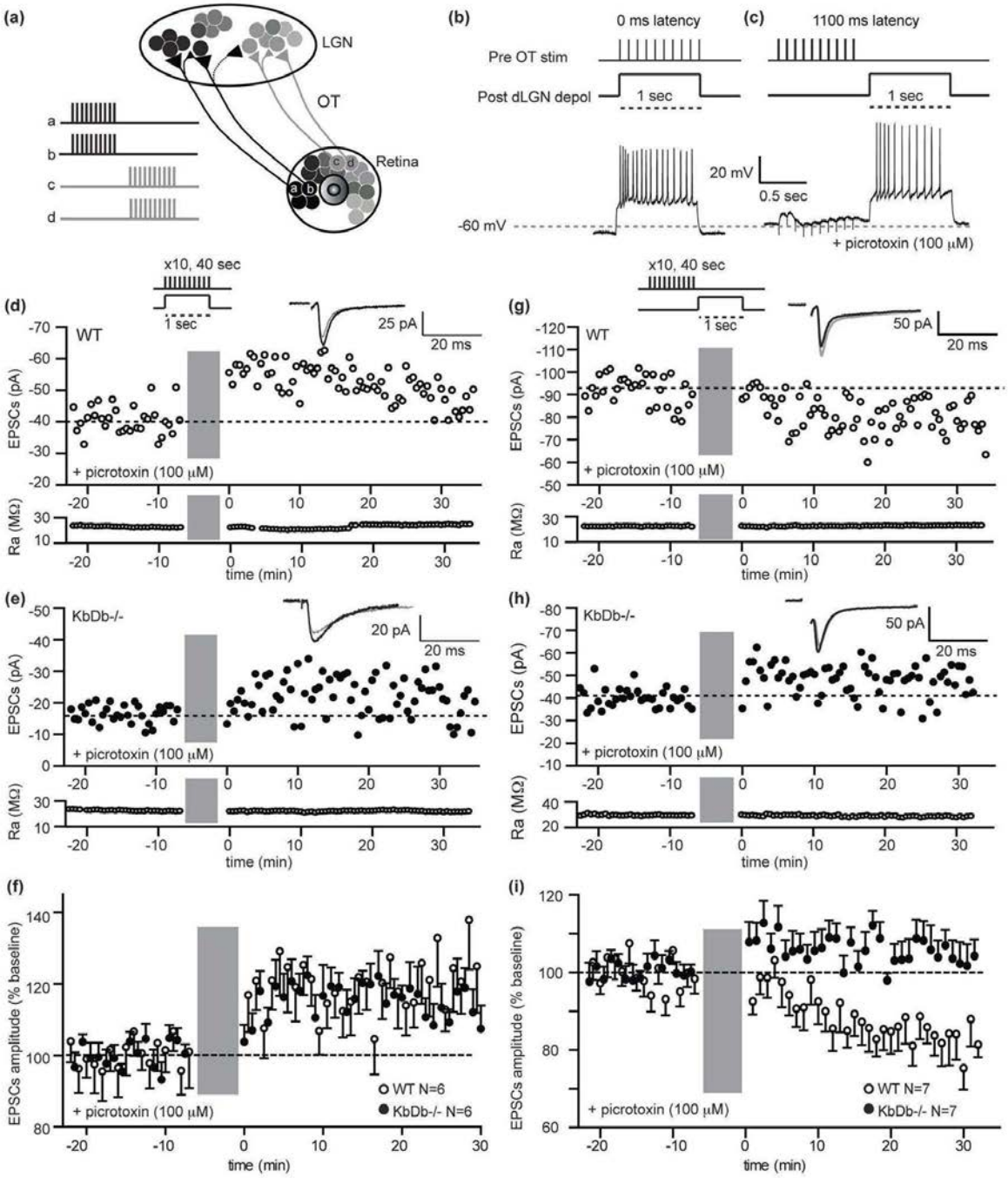

Figure 3. Impaired LTD but intact LTP at retinogeniculate synapses in KbDb–/– neurons induced with natural activity patterns. ***a***, Diagram illustrating basis for timing-dependent plasticity at developing RGC synapses. Inset, Spontaneous retinal waves propagate from "a, b" toward "c, d"; neighboring RGCs fire synchronously but asynchronously with respect to RGCs located elsewhere. Waves drive action potentials in postsynaptic LGN neurons with varying time delays between presynaptic and postsynaptic activity. Ages P8–P13 studied. ***b–c***, Top, Conditioning protocol for LTP (0 ms latency) (***b***) or LTD (1100 ms latency) (***c***). Bottom, example membrane potential changes recorded in LGN neuron during conditioning protocol. ***d–f,*** Intact LTP in KbDb–/– mice. Single experiment showing LTP in WT (***d***) and KbDb–/– (***e***) mice. EPSC peak amplitude vs time. ***f,*** Summary of all 0 ms latency experiments: EPSC peak amplitude (% change from baseline) vs time (n = 6/N = 6 for each; $p > 0.1$; *t*-test). ***g–i,*** Deficient LTD in KbDb–/– mice. Single experiment for WT (***g***) and KbDb–/– (***h***) mice. EPSC peak amplitude vs time. ***i,*** Summary of all 1100 ms latency experiments: EPSC peak amplitude (% change from baseline) vs time (n = 7/N = 7 for each; $p < 0.01$; *t*-test). Gray bars, induction period. Insets, Average EPSCs (30 traces) before (gray) and after (black) induction. ***f, i***, 1 min data binning. n = cells/N = animals; depol, depolarization; Ra, access resistance (MΩ); stim, stimulation. Reprinted with permission from Lee H et al. (2014), Figure 3. Copyright 2014, Nature Publishing Group.

effect ($p > 0.5$ at +40 mV), similar to WT neurons (Fig. 5*e*; Extended Data, Fig. 9*b*). Because the Ca^{2+} permeability of AMPA receptors is close to WT levels in KbDb–/–;NSEDb+ LGN, it is possible that LTD is also rescued. Indeed, the same asynchronous activity pattern that failed to induce LTD in KbDb–/– LGN (Fig. 3) induces robust LTD (15%; $p < 0.001$) in KbDb–/–;NSEDb+ neurons, similar to WT neurons (Figs. 5*f*,*g*). Together, these observations suggest that restoring expression of H2-Db in neurons is sufficient to rescue LTD at retinogeniculate synapses by decreasing the Ca^{2+} permeability of AMPA receptors.

Discussion

A major finding of this study is that the link between activity-dependent synapse pruning during development, and regulation of LTD and CP-AMPA receptors, requires neuronal MHCI function. It is notable that synapse elimination fails despite the fact that retinal waves and retinogeniculate basal synaptic transmission are intact. The persistence of multiple innervation in KbDb–/– LGN neurons is highly reminiscent of the immature synaptic connectivity in the LGN of younger WT mice (Chen and Regehr, 2000) as well as abnormal connectivity observed in the LGNs of dark-reared or TTX-treated WT mice (Hooks and Chen, 2006). Together, these considerations imply that H2-Db and H2-Kb act downstream of neural activity. In studying the synaptic plasticity at RGC synapses, we imposed plasticity induction protocols that mimic natural patterns of spiking activity present in the retinogeniculate system during synapse elimination and eye-specific segregation. Our observation that in KbDb–/– mice, LTD is impaired while LTP is intact can explain the failure in retinogeniculate synapse elimination: If synapses cannot undergo weakening, then they cannot be eliminated. Immunostaining for MHCI proteins H2-Db and H2-Kb is colocalized with synaptic markers in array tomography (Datwani et al., 2009) and at synapses in immunoelectron microscopy (Datwani et al., 2009; Needleman et al., 2010). Thus, these observations also argue strongly that H2-Db and/or H2-Kb at synapses regulate mechanisms of LTD, which in turn are required for synapse elimination. It would be useful to know whether other molecules implicated in RGC synapse elimination, such as C1q (Stevens et al., 2007), which colocalizes with H2-Db and H2-Kb at synapses (Datwani et al., 2009), also alter LTD or instead act downstream of MHCI to target already weakened synapses for removal.

The rescue experiments performed here imply that a single MHCI molecule—H2-Db, when expressed in neurons—is sufficient for functional synapse elimination and anatomical eye-specific segregation in the LGN. By crossing KbDb–/– mice to NSEDb+ transgenic mice, expression of H2-Db alone was restored to neurons but not elsewhere in the body, rescuing LTD, functional synapse elimination, Ca^{2+}-impermeable AMPA receptors, and structural remodeling at retinogeniculate synapses. Notably, these brain phenotypes are rescued even though the immune system is still impaired in KbDb–/–;NSEDb+ mice. Until this experiment, it was not known whether any one MHCI molecule is sufficient either *in vitro* or *in vivo*, nor has it been possible to separate the general effects of immune compromise from the absence of H2-Db and/or H2-Kb in neurons. Together, these observations argue for a key role for H2-Db in reading out endogenous activity patterns into a lasting structural framework. In the human genome,

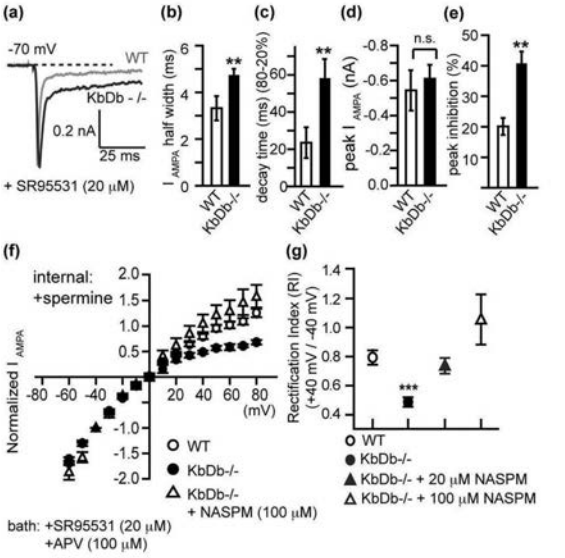

Figure 4. Increased CP-AMPA receptors at RGC synapses in KbDb–/– LGN. ***a–d***, Prolonged decay kinetics of I_{AMPA} in KbDb–/– LGN neurons. ***a,*** Average I_{AMPA} (5–10 EPSCs) for WT vs KbDb–/– LGN neurons ***b***, I_{AMPA} half width (ms), ***c***, I_{AMPA} decay time (ms) and ***d***, Peak amplitude (nA) for WT vs KbDb–/– mice (WT: n = 16/N = 4; KbDb–/–: n = 22/N = 5). ***e***, Increased inhibition of peak I_{AMPA} by NASPM in KbDb–/– (n = 13/N = 4) vs WT (n = 9/N = 3) mice (**$p < 0.01$; n.s., not significant; Mann-Whitney *U* test for ***b–c***). ***f,*** I_{AMPA} I–V curves (normalized to –40 mV). ***g***, Rectification index (RI) for WT (n = 14/N = 3), KbDb–/– (n = 9/N = 3), KbDb–/– +20 μM NASPM (n = 16/N = 4), or KbDb–/– +100 μM NASPM (n = 6/N = 2) (***$p < 0.001$ for WT vs KbDb–/–; $p > 0.05$ for WT vs KbDb–/– +NASPM [20 or 100 μM]; Mann-Whitney *U* test). Ages studied: P8–P13. See also Lee H et al, (2014) Extended Data, Fig. 7. n = cells/N = animals. Reprinted with permission from Lee H et al. (2014), Figure 4. Copyright 2014, Nature Publishing Group.

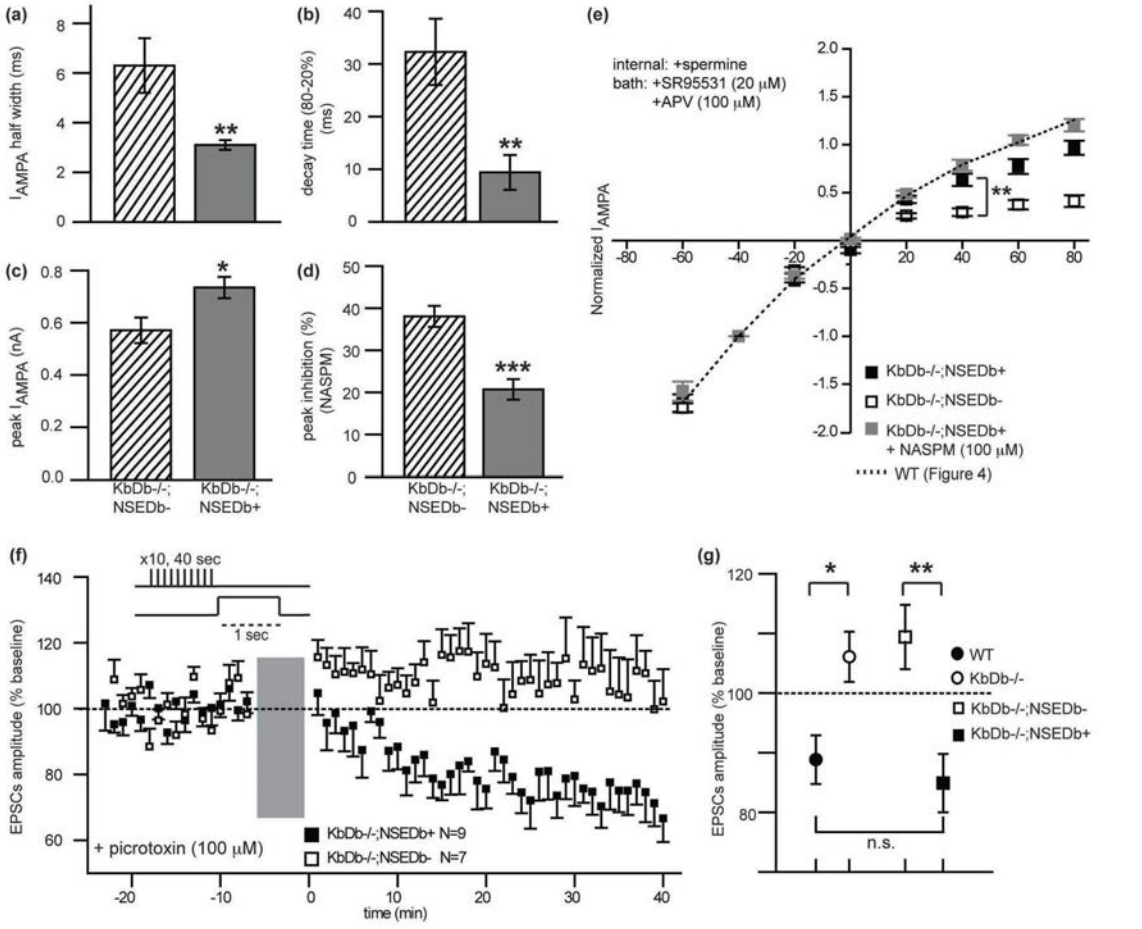

Figure 5. Neuronal expression of H2-Db restores Ca^{2+}-impermeable AMPA receptors and rescues LTD. ***a***, I_{AMPA} half width (ms), ***b***, I_{AMPA} decay time (ms), and ***c,*** Peak amplitude (nA) for KbDb–/–;NSEDb– (n = 9/N = 2) and KbDb–/–;NSEDb+ (n = 11/N = 4) LGN. ***d***, Reduced percentage inhibition of peak IAMPA by NASPM (100 μM) in KbDb–/–;NSEDb+ (n = 10/N = 3) compared with KbDb–/–;NSEDb– (n = 8/N = 2) LGN; *$p < 0.05$, **$p < 0.01$, ***$p < 0.001$; Mann–Whitney *U* test for ***a–d.*** ***e***, Rescue of I_{AMPA} linear I–V relationship in KbDb–/–;NSEDb+ LGN. Rectification index at +40 mV for KbDb–/–;NSEDb– (n = 11/N = 3) and KbDb–/–;NSEDb+ (n = 13/N = 5) LGN shows significant difference (**$p < 0.005$); in contrast, KbDb–/–;NSEDb+ (+NASPM) (n = 7/N = 3) is not significantly different from KbDb–/–;NSEDb+ ($p > 0.05$), Mann–Whitney *U* test. See also Extended Data, Fig. 9. Mean ± SEM. ***f, g,*** LTD rescued in KbDb;NSEDb+ LGN neurons. ***f,*** Ensemble average of all experiments at P8–P9 (Fig. 3). Gray bar, LTD induction period. 1 min data binning. ***g***, Average percentage change (mean ± SEM) for WT (N = 7), KbDb–/– (N = 7), or KbDb–/–;NSEDb– (N = 7) and KbDb–/–;NSEDb+ (N = 9) neurons. *$p < 0.05$, **$p < 0.01$, n.s., not significant; *t*-test. Ages studied: P8–P13. n = cells/N = animals. Reprinted with permission from Lee H et al. (2014), Figure 5. Copyright 2014, Nature Publishing Group.

as in mice, the MHCI (human leukocyte antigen) locus is large and highly polymorphic. Recent genome-wide association studies have consistently linked specific single nucleotide polymorphisms in MHCI to schizophrenia (Stefansson et al., 2009; Ripke et al., 2013). Our observations offer possible mechanistic insight: Alterations in expression levels of specific MHCIs at neuronal synapses could trigger changes in activity-dependent plasticity and synaptic pruning during critical periods of human development, generating lasting alterations in circuits and behavior.

Methods Summary

KbDb–/– mice were maintained on C57BL/6 backgrounds. Crosses of these two lines generated KbDb–/–;NSEDb+ mice plus littermate controls. Electrophysiological recordings were made from LGN neurons by cutting parasagittal brain slices containing dorsal LGN and optic tract; synaptic transmission and degree of innervation were assessed as previously described (Chen and Regehr, 2000). For plasticity experiments at retinogeniculate synapses, perforated patch-clamp technique and induction protocols with natural activity patterns were used (Butts et al., 2007). Multielectrode array

NOTES

recordings of retinal waves and anatomical labeling of retinogeniculate projections to determine status of eye-specific segregation were carried out according to Torborg et al. (2005) and Datwani et al. (2009). Pharmacological investigation of CP-AMPA receptors was made according to Liu and Cull-Candy (2000). All experiments were conducted and analyzed blind to genotype except in Figure 4 (in which genotype was obvious to the experimenter because of phenotype). Sample sizes were chosen for each experiment to reach statistical significance ($p \leq 0.05$).

Acknowledgments

All experimental protocols were approved by Stanford University Animal Care and Use Committees. KbDb–/– mice were generously provided by H. Ploegh (Vugmeyster et al., 1998) and NSEDb mice by Michael B.A. Oldstone (Rall et al., 1995). We thank members of the Shatz Lab for helpful comments. For technical assistance, thanks to N. Sotelo-Kury, C. Chechelski, and P. Kemper. For training in retinogeniculate slice methods, we thank Dr. Chinfei Chen (Boston Children's Hospital, Harvard Medical School) and Drs. Patrick Kanold and Dan Butts (University of Maryland, College Park). This work was supported by National Institutes of Health (NIH) Grants R01 MH071666 and EY02858; the G. Harold and Leila Y. Mathers Charitable Foundation (C.J.S.); NIH Grant RO1 EY13528 (M.B.F.); National Defense Science and Engineering Graduate and National Science Foundation (NSF) Graduate Research Fellowships (J.D.A.); and an NSF Predoctoral Fellowship (L.A.K.). This chapter was modified from a previously published version: Lee, et al. (2014) Synapse elimination and learning rules coregulated by MHC Class I H2-Db. Nature 509:195–200. Copyright 2014, Nature Publishing Group. Supplementary materials, including Extended Data and complete Methods, are available at https://www.ncbi.nlm.nih.gov/pmc/articles/PMC4016165.

References

Ackman JB, Burbridge, TJ, Crair MC (2012) Retinal waves coordinate patterned activity throughout the developing visual system. Nature 490:219–225.

Bastrikova N, Gardner GA, Reece JM, Jeromin A, Dudek SM (2008) Synapse elimination accompanies functional plasticity in hippocampal neurons. Proc Natl Acad Sci USA 105:3123–3127.

Bjartmar L, Huberman AD, Ullian EM, Rentería RC, Liu X, Xu W, Prezioso J, Susman MW, Stellwagen D, Stokes CC, Cho R, Worley P, Malenka RC, Ball S, Peachey NS, Copenhagen D, Chapman B, Nakamoto M, Barres BA, Perin MS (2006) Neuronal pentraxins mediate synaptic refinement in the developing visual system. J Neurosci 26:6269–6281.

Butts DA, Kanold PO, Shatz CJ (2007) A burst-based "Hebbian" learning rule at retinogeniculate synapses links retinal waves to activity-dependent refinement. PLoS Biol 5:e61.

Chen C, Regehr WG (2000) Developmental remodeling of the retinogeniculate synapse. Neuron 28:955–966.

Corriveau RA, Huh GS, Shatz CJ (1998) Regulation of class I MHC gene expression in the developing and mature CNS by neural activity. Neuron 21:505–520.

Cull-Candy S, Kelly L, Farrant M (2006) Regulation of Ca^{2+}-permeable AMPA receptors: synaptic plasticity and beyond. Curr Opin Neurobiol 16:288–297.

Datwani A, McConnell MJ, Kanold PO, Micheva KD, Busse B, Shamloo M, Smith SJ, Shatz CJ (2009) Classical MHCI molecules regulate retinogeniculate refinement and limit ocular dominance plasticity. Neuron 64:463–470.

Feller MB, Wellis DP, Stellwagen D, Werblin FS, Shatz CJ (1996) Requirement for cholinergic synaptic transmission in the propagation of spontaneous retinal waves. Science 272:1182–1187.

Glynn MW, Elmer BM, Garay PA, Liu XB, Needleman LA, El-Sabeawy F, McAllister AK (2011) MHCI negatively regulates synapse density during the establishment of cortical connections. Nat Neurosci 14:442–451.

Goel A, Jiang B, Xu LW, Song L, Kirkwood A, Lee HK (2006) Cross-modal regulation of synaptic AMPA receptors in primary sensory cortices by visual experience. Nat Neurosci 9:1001–1003.

Hohnke CD, Oray S, Sur M (2000) Activity-dependent patterning of retinogeniculate axons proceeds with a constant contribution from AMPA and NMDA receptors. J Neurosci 20:8051–8060.

NOTES

Hooks BM, Chen C (2006) Distinct roles for spontaneous and visual activity in remodeling of the retinogeniculate synapse. Neuron 52:281–291.

Huberman AD, Feller MB, Chapman B (2008) Mechanisms underlying development of visual maps and receptive fields. Annu Rev Neurosci 31:479–509.

Huh GS, Boulanger LM, Du H, Riquelme PA, Brotz TM, Shatz CJ (2000) Functional requirement for class I MHC in CNS development and plasticity. Science 290:2155–2159.

Isaac JT, Ashby MC, McBain CJ (2007) The role of the GluR2 subunit in AMPA receptor function and synaptic plasticity. Neuron 54:859–871.

Jia Z, Agopyan N, Miu P, Xiong Z, Henderson J, Gerlai R, Taverna FA, Velumian A, MacDonald J, Carlen P, Abramow-Newerly W, Roder J (1996) Enhanced LTP in mice deficient in the AMPA receptor GluR2. Neuron 17:945–956.

Lee H, Kirkby L, Brott BK, Adelson JD, Cheng S, Feller MB, Datwani A, Shatz CJ (2004) Synapse elimination and learning rules coregulated by MHC class I H2-Db. Nature 509:195–200.

Liu SQ, Cull-Candy SG (2000) Synaptic activity at calcium-permeable AMPA receptors induces a switch in receptor subtype. Nature 405:454–458.

Malenka RC, Bear MF (2004) LTP and LTD: an embarrassment of riches. Neuron 44:5–21.

Meister M, Wong RO, Baylor DA, Shatz CJ (1991) Synchronous bursts of action potentials in ganglion cells of the developing mammalian retina. Science 252:939–943.

Mooney R, Madison DV, Shatz CJ (1993) Enhancement of transmission at the developing retinogeniculate synapse. Neuron 10:815–825.

Mooney R, Penn AA, Gallego R, Shatz CJ (1996) Thalamic relay of spontaneous retinal activity prior to vision. Neuron 17:863–874.

Mu Y, Poo MM (2006) Spike timing-dependent LTP/LTD mediates visual experience–dependent plasticity in a developing retinotectal system. Neuron 50:115–125.

Needleman LA, Liu XB, El-Sabeawy F, Jones EG, McAllister AK (2010) MHC class I molecules are present both pre- and postsynaptically in the visual cortex during postnatal development and in adulthood. Proc Natl Acad Sci USA 107:16999–17004.

Penn AA, Riquelme PA, Feller MB, Shatz CJ (1998) Competition in retinogeniculate patterning driven by spontaneous activity. Science 279:2108–2112.

Rall GF, Mucke L, Oldstone MB (1995) Consequences of cytotoxic T lymphocyte interaction with major histocompatibility complex class I–expressing neurons *in vivo*. J Exp Med 182:1201–1212.

Ripke S, O'Dushlaine C, Chambert K, Moran JL, Kähler AK, Akterin S, Bergen SE, Collins AL, Crowley JJ, Fromer M, Kim Y, Lee SH, Magnusson PK, Sanchez N, Stahl EA, Williams S, Wray NR, Xia K, Bettella F, Borglum AD, et al. (2013) Genome-wide association analysis identifies 13 new risk loci for schizophrenia. Nat Genet 45:1150–1159.

Shah RD, Crair MC (2008) Retinocollicular synapse maturation and plasticity are regulated by correlated retinal waves. J Neurosci 28:292–303.

Shatz CJ, Kirkwood PA (1984) Prenatal development of functional connections in the cat's retinogeniculate pathway. J Neurosci 4:1378–1397.

Shatz CJ (1996) Emergence of order in visual system development. Proc Natl Acad Sci USA 93:602–608.

Stefansson H, Ophoff RA, Steinberg S, Andreassen OA, Cichon S, Rujescu D, Werge T, Pietiläinen OP, Mors O, Mortensen PB, Sigurdsson E, Gustafsson O, Nyegaard M, Tuulio-Henriksson A, Ingason A, Hansen T, Suvisaari J, Lonnqvist J, Paunio T, Børglum AD, et al. (2009) Common variants conferring risk of schizophrenia. Nature 460:744–747.

Stevens B, Allen NJ, Vazquez LE, Howell GR, Christopherson KS, Nouri N, Micheva KD, Mehalow AK, Huberman AD, Stafford B, Sher A, Litke AM, Lambris JD, Smith SJ, John SW, Barres BA (2007) The classical complement cascade mediates CNS synapse elimination. Cell 131:1164–1178.

Stevens CF, Wang Y (1994) Changes in reliability of synaptic function as a mechanism for plasticity. Nature 371:704–707.

Torborg CL, Feller MB (2004) Unbiased analysis of bulk axonal segregation patterns. J Neurosci Methods 135:17–26.

Torborg CL, Hansen KA, Feller MB (2005) High frequency, synchronized bursting drives eye-specific segregation of retinogeniculate projections. Nat Neurosci 8:72–78.

Toyoda H, Wu LJ, Zhao MG, Xu H, Jia Z, Zhuo M (2007) Long-term depression requires postsynaptic AMPA GluR2 receptor in adult mouse cingulate cortex. J Cell Physiol 211:336–343.

Vugmeyster Y, Glas R, Pérarnau B, Lemonnier FA, Eisen H, Ploegh H (1998) Major histocompatibility complex (MHC) class I K^bD^b–/– deficient mice possess functional CD8+ T cells and natural killer cells. Proc Natl Acad Sci USA 95:12492–12497.

Weliky M, Katz LC (1999) Correlational structure of spontaneous neuronal activity in the developing lateral geniculate nucleus *in vivo*. Science 285:599–604.

Wong RO, Meister M, Shatz CJ (1993) Transient period of correlated bursting activity during development of the mammalian retina. Neuron 11:923–938.

Yuste R, Bonhoeffer T (2001) Morphological changes in dendritic spines associated with long-term synaptic plasticity. Annu Rev Neurosci 24:1071–1089.

Zhang J, Ackman JB, Xu HP, Crair MC (2011) Visual map development depends on the temporal pattern of binocular activity in mice. Nat Neurosci 15:298–307.

Zhou Q, Homma KJ, Poo MM (2004) Shrinkage of dendritic spines associated with long-term depression of hippocampal synapses. Neuron 44:749–757.

Ziburkus J, Dilger EK, Lo FS, Guido W (2009) LTD and LTP at the developing retinogeniculate synapse. J Neurophysiol 102:3082–3090.

NOTES